VI International Conference on Computational Methods for Coupled Problems in Science and Engineering
COUPLED PROBLEMS 2015
B. Schrefler, E. Oñate and M. Papadrakakis(Eds)

CONVERGENCE SPEED OF COUPLING ITERATIONS FOR THE UNSTEADY TRANSMISSION PROBLEM

AZAHAR MONGE* AND PHILIPP BIRKEN*

*Centre for Mathematical Sciences
Lund University
Box 118, 22100, Lund, Sweden
e-mail: azahar.monge@na.lu.se, web page: http://www.maths.lu.se/staff/azahar-monge

Key words: Thermal Fluid Structure Interaction, Coupled Problems, Transmission Problem, Fixed Point Iteration, Dirichlet-Neumann Iteration

Abstract. We present an estimate for the convergence rate of the Dirichlet-Neumann iteration for the discretized unsteady transmission problem. Specifically, we consider the coupling of two heat equations on two identical squared domains. The Laplacian is discretized by second order central finite differences and the implicit Euler method is used for the time discretization. For the semidiscrete case, Henshaw and Chad provided in 2009 a method to analyse stability and convergence speed based on applying the continuous Fourier transform to the semi-discretized equations. Numerical results for the fully discrete case show differences, which is why we propose a complementary analysis based on approximating the spectral radius of the iteration matrix. Numerical results are presented to illustrate the analysis.

1 INTRODUCTION

Thermal fluid structure interaction occurs when a heat flux from a fluid leads to temperature changes in a structure or vice versa. Examples for this are cooling of gas-turbine blades, cooling of rocket thrust chambers [9], thermal anti-icing systems of airplanes [3], supersonic reentry of vehicles from space [8, 10] or gas quenching [6, 14].

Unsteady thermal fluid structure interaction is modelled using two partial differential equations describing a fluid and a structure on different domains. The equations are coupled at an interface to model the heat transfer between fluid and structure. For the solution of a coupled problem, two general approaches can be distinguished. In a partitioned approach [4], different codes for the sub-problems are used and the coupling is done by a master program which calls interface functions of the other codes. This allows to use existing software for each sub-problem, in contrast to a monolithic approach, where a new code is tailored for the coupled equations. The standard partitioned algorithm is

the Dirichlet-Neumann iteration, where the PDEs are solved separately using Dirichlet, respectively Neumann boundary conditions with data given from the solution of the other problem. This iteration has been analyzed and a convergence condition is given by [12], but convergence rates have not been computed.

Henshaw and Chad provided in [7] a method to analyse stability and convergence speed of the Dirichlet-Neumann iteration for the thermal transmission problem based on applying the continuous Fourier transform to the semi-discretized equations. Their result depends on the thermal conductivities and diffusivities of the materials. However, in the fully-discrete case we observe that the iteration converges much faster [2]. Therefore, we propose a complementary stability and convergence study for this case.

In this paper we consider the transmission problem because it is a basic building block in fluid structure interaction. In particular, we consider the coupling of two heat equations on two identical squared domains. The Laplacian is discretized by second order central finite differences and the implicit Euler method is used for the time discretization.

To study the convergence behaviour of this problem, we reformulate the fully-discrete iteration as a system of algebraic equations. For each domain, we have a matrix describing the discretization of the Laplacian and a matrix describing the coupling conditions. This leads us to a linear coupled system of equations with sparse block tridiagonal matrices. Using the Schur complement [15], the exact iteration matrix can be written down. However, the spectral radius of that is too difficult to compute. We therefore present an estimate based on approximating the iteration matrix by its block diagonal because the iteration matrix is a strictly diagonally dominant matrix.

An outline of the paper now follows. In Section 2, we define the problem to be solved in terms of the partial differential equations, boundary conditions and interface conditions. We also give a description of the discretization. In Section 3, we explain how to solve the model problem using a fixed point iteration. Our stability analysis for the fully-discretized case of the model problem using Dirichlet-Neumann interface conditions is presented in Section 4. In Section 5, we present numerical results that show the theoretical stability analysis. Conclusions are given in the final section.

2 MODEL PROBLEM AND DISCRETIZATION

The unsteady transmission problem is as follows, where we consider a domain Ω which is cut into two subdomains $\Omega = \Omega_1 \cup \Omega_2$ with transmission conditions at the interface $\Gamma = \Omega_1 \cap \Omega_2$:

$$\begin{aligned}
\frac{\partial u_m(\mathbf{x},t)}{\partial t} + D_m \Delta u_m(\mathbf{x},t) = f(\mathbf{x}), \quad t \in [t_0, t_f] \quad \mathbf{x} = (x,y) \in \Omega_m \subset \mathbb{R}^2, \ m = 1,2 \\
u_m(\mathbf{x},t) = 0, \quad t \in [t_0, t_f], \quad \mathbf{x} \in \partial\Omega_m \backslash \Gamma \\
u_1(\mathbf{x},t) = u_2(\mathbf{x},t), \quad \mathbf{x} \in \Gamma \\
K_1 \partial_x u_1(\mathbf{x},t) \cdot \mathbf{n} = K_2 \partial_x u_2(\mathbf{x},t) \cdot \mathbf{n}, \quad \mathbf{x} \in \Gamma \\
u_m(\mathbf{x},0) = g_m(\mathbf{x}), \quad \mathbf{x} \in \Omega_m
\end{aligned} \tag{1}$$

The constants K_1 and K_2 describe the thermal conductivities of the materials on Ω_1 and Ω_2 respectively. Analogously, D_1 and D_2 represent the thermal diffusivities of the materials.

For this study, we use $\Omega_1 = [0,1] \times [0,1]$, $\Omega_2 = [1,2] \times [0,1]$ and

$$\begin{aligned} f(x,y) = \sin \pi y^2 (\pi \cos \frac{\pi}{2} x^2 - \pi^2 x^2 \sin \frac{\pi}{2} x^2) \\ + \sin \frac{\pi}{2} x^2 (2\pi \cos \pi y^2 - 4\pi^2 y^2 \sin \pi y^2). \end{aligned} \tag{2}$$

This was chosen such that the exact solution is

$$u(x,y) = \sin \pi y^2 \sin \frac{\pi}{2} x^2, \tag{3}$$

which satisfies the boundary conditions.

We discretize this problem using second order central differences for the Laplacian with a constant mesh width of $\Delta x = \Delta y$. For the time discretization we use the implicit Euler method. All linear systems are solved using CG.

2.1 Space Discretization

Let's first discretize the equation $D_1 \Delta u_1(x,y) = f(x,y)$ on Ω_1 with Dirichlet boundary conditions at the interface Γ. Consider $u_1(x_i, y_j) \approx u_{1,i,j}$ for $i = 0, ..N_x$, $j = 0, .., N_x + 1$ and $\Delta x = \Delta y = 1/(N_x + 1)$. We use the following second order central difference to approximate the second order spatial derivatives,

$$u_{1,xx}(x_i, y_j) \approx \frac{1}{\Delta x^2}(u_{1,i+1,j} - 2u_{1,i,j} + u_{1,i-1,j}), \tag{4}$$

$$u_{1,yy}(x_i, y_j) \approx \frac{1}{\Delta x^2}(u_{1,i,j+1} - 2u_{1,i,j} + u_{1,i,j-1}). \tag{5}$$

These approximations lead us to the following linear system,

$$\mathbf{A}_1 \mathbf{u}_1 + \mathbf{f}_1 = 0, \tag{6}$$

where $\mathbf{A}_1 \in \mathbb{R}^{N_x \cdot N_x \times N_x \cdot N_x}$ and $\mathbf{u}_1$, $\mathbf{f}_1 \in \mathbb{R}^{N_x \cdot N_x \times 1}$. $\mathbf{A}_1$ is given by

$$\mathbf{A}_1 := -\frac{D_1}{\Delta x^2} \begin{pmatrix} \tilde{\mathbf{A}} & \mathbf{I} & & \mathbf{0} \\ \mathbf{I} & \tilde{\mathbf{A}} & \ddots & \\ & \ddots & \ddots & \mathbf{I} \\ \mathbf{0} & & \mathbf{I} & \tilde{\mathbf{A}} \end{pmatrix} \quad \text{where} \quad \tilde{\mathbf{A}} := \begin{pmatrix} -4 & 1 & & 0 \\ 1 & -4 & \ddots & \\ & \ddots & \ddots & 1 \\ 0 & & 1 & -4 \end{pmatrix}_{N_x \times N_x} \tag{7}$$

and $\mathbf{I}$ is the identity matrix. Note that each block of the matrix $\mathbf{A}_1$ has size $N_x \times N_x$.

Finally, on the right boundary we have to add a matrix $\mathbf{P}$ describing the Dirichlet coupling conditions at the interface. The full discretization is described as follows,

$$\mathbf{A}_1 \mathbf{u}_1 + \mathbf{P} \mathbf{u}_2 + \mathbf{f}_1 = 0,$$

where $\mathbf{P} \in \mathbb{R}^{N_x \cdot N_x \times (N_x+1)\cdot N_x}$ and is defined by

$$\mathbf{P} = \frac{D_1}{\Delta x^2} \begin{pmatrix} \mathbf{0} & \mathbf{0} \\ \mathbf{I} & \mathbf{0} \end{pmatrix}. \tag{8}$$

The bottom left block of the matrix $\mathbf{P}$ has size $N_x \times N_x$.

On the other hand, we also need to discretize the equation $D_2 \Delta u_2(x,y) = f(x,y)$ on Ω_2 with Neumann boundary conditions at the interface Γ and Dirichlet boundary conditions on $\partial\Omega_2 \backslash \Gamma$. The discretization for the interior points of the grid is the same as for Ω_1. Therefore, we only need to develop the discretization of this equation on the left boundary.

We discretize the Neumann boundary conditions at the interface using forward finite differences:

$$K_1 \partial u_1(x_{N_x+1}, y_j) \cdot \mathbf{n} \approx \frac{K_1(u_{1,N_x,j} - u_{1,N_x+1,j})}{\Delta x} \quad \text{and} \tag{9}$$

$$K_2 \partial u_2(x_0, y_j) \cdot \mathbf{n} \approx \frac{K_2(u_{2,0,j} - u_{2,1,j})}{\Delta x} \quad \text{for} \quad j = 0, .., N_x + 1. \tag{10}$$

In general, the entire discretization looks as follows,

$$\mathbf{A}_2 \mathbf{u}_2 + \mathbf{D}\mathbf{u}_1 + \mathbf{f}_2 = 0, \tag{11}$$

where $\mathbf{A}_2 \in \mathbb{R}^{(N_x+1)\cdot N_x \times (N_x+1)\cdot N_x}$, $\mathbf{D} \in \mathbb{R}^{(N_x+1)\cdot N_x \times N_x \cdot N_x}$ is the discrete normal derivative at the interface and $\mathbf{u}_1$, $\mathbf{u}_2$, $\mathbf{f}_2 \in \mathbb{R}^{(N_x+1)\cdot N_x \times 1}$. $\mathbf{A}_2$ is given by

$$\mathbf{A}_2 := -\frac{D_2}{\Delta x^2} \begin{pmatrix} \hat{\mathbf{A}} & \mathbf{I} & & \mathbf{0} \\ \mathbf{I} & \tilde{\mathbf{A}} & \ddots & \\ & \ddots & \ddots & \mathbf{I} \\ \mathbf{0} & & \mathbf{I} & \tilde{\mathbf{A}} \end{pmatrix} \quad \text{where} \quad \hat{\mathbf{A}} := \begin{pmatrix} -3 & 1 & & 0 \\ 1 & -3 & \ddots & \\ & \ddots & \ddots & 1 \\ 0 & & 1 & -3 \end{pmatrix}_{N_x \times N_x}. \tag{12}$$

Note that each block of the matrix $\mathbf{A}_2$ has size $N_x \times N_x$. $\mathbf{D}$ is described as follows,

$$\mathbf{D} = \frac{D_2}{\Delta x^2} \begin{pmatrix} \mathbf{0} & \tilde{\mathbf{D}} \\ \mathbf{0} & \mathbf{0} \end{pmatrix} \quad \text{where} \quad \tilde{\mathbf{D}} = \frac{K_1}{K_2} \begin{pmatrix} \mathbf{I} & -\mathbf{I} \end{pmatrix}_{N_x \times 2N_x}. \tag{13}$$

2.2 Time Discretization

As we said before, we use the implicit Euler method for the time discretization of (1). In order to simplify the analysis, we assume that $\mathbf{f}_1 = \mathbf{f}_2 \equiv \mathbf{0}$ without loss of generality. Therefore, one can rewrite the time dependent transmission problem as the coupled equations

$$\begin{aligned} \dot{\mathbf{u}}_1 &= \mathbf{A}_1 \mathbf{u}_1 + \mathbf{P}\mathbf{u}_2, \\ \dot{\mathbf{u}}_2 &= \mathbf{A}_2 \mathbf{u}_2 + \mathbf{D}\mathbf{u}_1, \end{aligned} \tag{14}$$

where $\mathbf{A}_1$ corresponds to the space discretization on Ω_1, $\mathbf{A}_2$ to the space discretization on Ω_2, $\mathbf{P}$ to the Dirichlet boundary conditions mapping from Ω_2 to Ω_1 and $\mathbf{D}$ to the Neumann boundary conditions mapping from Ω_1 to Ω_2.

Applying the implicit Euler method to the system (14), we get

$$\mathbf{u}_1^{n+1} = \mathbf{u}_1^n - \Delta t(\mathbf{A}_1\mathbf{u}_1^{n+1} + \mathbf{P}\mathbf{u}_2^{n+1}), \tag{15}$$
$$\mathbf{u}_2^{n+1} = \mathbf{u}_2^n - \Delta t(\mathbf{A}_2\mathbf{u}_2^{n+1} + \mathbf{D}\mathbf{u}_1^{n+1}), \tag{16}$$

with the time step size Δt fixed.

3 FIXED POINT ITERATION

We now employ a standard Dirichlet-Neumann iteration to solve the discrete system (15)-(16). This corresponds to alternately solving the problems (15) and (16), where problem (15) corresponds to a discretization of the transmission problem (1) on Ω_1 only with Dirichlet data on Γ given by $\mathbf{u}_2$ on the coupling interface and problem (16) corresponds to a discretization of (1) on Ω_2 only with Neumann data on Γ given by the discrete normal derivative of $\mathbf{u}_1$ on Γ. This iteration is also known as Gauss-Seidel process [12].

Applying this to (15)-(16), one gets for the k-th iteration

$$\mathbf{u}_1^{n+1,k+1} = \mathbf{u}_1^n - \Delta t(\mathbf{A}_1\mathbf{u}_1^{n+1,k+1} + \mathbf{P}\mathbf{u}_2^{n+1,k}), \tag{17}$$
$$\mathbf{u}_2^{n+1,k+1} = \mathbf{u}_2^n - \Delta t(\mathbf{A}_2\mathbf{u}_2^{n+1,k+1} + \mathbf{D}\mathbf{u}_1^{n+1,k+1}), \tag{18}$$

with some initial condition, here $\mathbf{u}_2^{n+1,0} = \mathbf{u}_2^n$.

The iteration is terminated according to the standard criterion $\|\mathbf{u}^{k+1} - \mathbf{u}^k\| \leq \tau$ [1].

4 ANALYSIS

In this section we present the convergence analysis for the semi discrete and the fully discrete case of the model problem.

4.1 Semi Discrete Case

Here, one applies the implicit Euler method for the time discretization on both equations in (1) but keeps the space continuous. Then, Henshaw and Chand applied in [7] the Fourier transform in space in order to transform the second order derivatives into algebraic expressions. This converts the partial differential equations into a system of purely algebraic equations. Once we have a coupled system of algebraic equations, we can insert one into the other one and obtain the amplification factor β which is approximated by

$$\beta \approx \frac{K_1}{K_2}\sqrt{\frac{D_2}{D_1}}. \tag{19}$$

4.2 Discrete Case

To analyze the iteration (17)-(18), we isolate the term $\mathbf{u}_i^{n+1,k+1}$ for $i = 1, 2$ in both equations:

$$\mathbf{u}_1^{n+1,k+1} = (\mathbf{I} + \Delta t \mathbf{A}_1)^{-1}(\mathbf{u}_1^n - \Delta t \mathbf{P}\mathbf{u}_2^{n+1,k}), \tag{20}$$
$$\mathbf{u}_2^{n+1,k+1} = (\mathbf{I} + \Delta t \mathbf{A}_2)^{-1}(\mathbf{u}_2^n - \Delta t \mathbf{D}\mathbf{u}_1^{n+1,k+1}). \tag{21}$$

Now we insert (20) into (21)

$$\begin{aligned}\mathbf{u}_2^{n+1,k+1} &= (\mathbf{I} + \Delta t \mathbf{A}_2)^{-1}(\mathbf{u}_2^n - \Delta t \mathbf{D}(\mathbf{I} + \Delta t \mathbf{A}_1)^{-1}(\mathbf{u}_1^n - \Delta t \mathbf{P}\mathbf{u}_2^{n+1,k})) \\ &= (\mathbf{I} + \Delta t \mathbf{A}_2)^{-1}\mathbf{u}_2^n - (\mathbf{I} + \Delta t \mathbf{A}_2)^{-1}\Delta t \mathbf{D}(\mathbf{I} + \Delta t \mathbf{A}_1)^{-1}\mathbf{u}_1^n \\ &\quad + (\mathbf{I} + \Delta t \mathbf{A}_2)^{-1}\Delta t \mathbf{D}(\mathbf{I} + \Delta t \mathbf{A}_1)^{-1}\Delta t \mathbf{P}\mathbf{u}_2^{n+1,k}.\end{aligned} \tag{22}$$

To prove convergence, one needs to show that the norm of the iteration matrix $\mathbf{M} = (\mathbf{I}+\Delta t\mathbf{A}_2)^{-1}\Delta t\mathbf{D}(\mathbf{I}+\Delta t\mathbf{A}_1)^{-1}\Delta t\mathbf{P}$ is smaller than 1 in some norm. Here we choose $\|\cdot\|_2$.

The first natural idea when facing the problem of computing $\|\mathbf{M}\|_2$ is to use the following basic norm property:

$$\|\mathbf{M}\|_2 \leq \Delta t^2 \|(\mathbf{I} + \Delta t \mathbf{A}_2)^{-1}\|_2 \|\mathbf{D}\|_2 \|(\mathbf{I} + \Delta t \mathbf{A}_1)^{-1}\|_2 \|\mathbf{P}\|_2. \tag{23}$$

However, the inequality in (23) is too coarse and the right hand side of the previous expression is way bigger than 1. Any other combination of breaking $\|\mathbf{M}\|_2$ lead us to the same situation. In conclusion, in order to compute $\|\mathbf{M}\|_2$ we need to compute the iteration matrix $\mathbf{M}$ and apply the norm afterwards.

The iteration matrix $\mathbf{M}$ is not easy to compute for different reasons. First of all, the matrices $\mathbf{I} + \Delta t \mathbf{A}_1$ and $\mathbf{I} + \Delta t \mathbf{A}_2$ are sparse block tridiagonal matrices, and consequently, their inverses are not a straight forward computation. A block-by-block algorithm for inverting a block tridiagonal matrix is explained in [13]. However, the algorithm is based on the iterative application of the Schur complement [15], and it results in a sequence of block matrices and inverses of block matrices that it is impossible to compute exactly. Moreover, the diagonal block matrices of $\mathbf{I} + \Delta t \mathbf{A}_1$ and $\mathbf{I} + \Delta t \mathbf{A}_2$ are tridiagonal matrices but their inverses are full matrices [5] which does not help for computing $\mathbf{M}$.

Due to these difficulties, we propose here to approximate $\mathbf{M}$. One can observe that $\mathbf{I}+\Delta t\mathbf{A}_1$ and $\mathbf{I}+\Delta t\mathbf{A}_2$ are strictly diagonally dominant matrices, and therefore, we propose to approximate them by the their block diagonal. Explicitly, if we define $\tilde{\mathbf{A}}_1 := \Delta x^2 \mathbf{A}_1$, we approximate

$$\mathbf{I} + \Delta t \mathbf{A}_1 = \mathbf{I} + \frac{D_1 \Delta t}{\Delta x^2}\tilde{\mathbf{A}}_1 \approx \text{blockdiag}\left(\mathbf{I} + \frac{D_1 \Delta t}{\Delta x^2}\tilde{\mathbf{A}}_1\right) = \begin{pmatrix} \mathbf{A} & & \mathbf{0} \\ & \ddots & \\ \mathbf{0} & & \mathbf{A} \end{pmatrix}, \tag{24}$$

where $\mathbf{A}$ is defined by (compare with (7))

$$\mathbf{A} := \begin{pmatrix} 1+4\frac{D_1\Delta t}{\Delta x^2} & -\frac{D_1\Delta t}{\Delta x^2} & & 0 \\ -\frac{D_1\Delta t}{\Delta x^2} & 1+4\frac{D_1\Delta t}{\Delta x^2} & \ddots & \\ & \ddots & \ddots & -\frac{D_1\Delta t}{\Delta x^2} \\ 0 & & -\frac{D_1\Delta t}{\Delta x^2} & 1+4\frac{D_1\Delta t}{\Delta x^2} \end{pmatrix}_{N_x\times N_x}.$$

Analogously, if we define $\tilde{\mathbf{A}}_2 := \Delta x^2 \mathbf{A}_2$, we approximate

$$\mathbf{I} + \Delta t \mathbf{A}_2 = \mathbf{I} + \frac{D_2\Delta t}{\Delta x^2}\tilde{\mathbf{A}}_2 \approx \text{blockdiag}\left(\mathbf{I} + \frac{D_2\Delta t}{\Delta x^2}\tilde{\mathbf{A}}_2\right) = \begin{pmatrix} \mathbf{B} & & & \mathbf{0} \\ & \mathbf{A} & & \\ & & \ddots & \\ \mathbf{0} & & & \mathbf{A} \end{pmatrix}, \quad (25)$$

where $\mathbf{B}$ is defined by (compare with (12))

$$\mathbf{B} := \begin{pmatrix} 1+3\frac{D_2\Delta t}{\Delta x^2} & -\frac{D_2\Delta t}{\Delta x^2} & & 0 \\ -\frac{D_2\Delta t}{\Delta x^2} & 1+3\frac{D_2\Delta t}{\Delta x^2} & \ddots & \\ & \ddots & \ddots & -\frac{D_2\Delta t}{\Delta x^2} \\ 0 & & -\frac{D_2\Delta t}{\Delta x^2} & 1+3\frac{D_2\Delta t}{\Delta x^2} \end{pmatrix}_{N_x\times N_x}.$$

Observe that $\mathbf{A}$ and $\mathbf{B}$ are nonsingular and thus [11]

$$\|\mathbf{A}^{-1}\|_2 = \frac{1}{\sigma_{\min}(\mathbf{A})}, \quad \|\mathbf{B}^{-1}\|_2 = \frac{1}{\sigma_{\min}(\mathbf{B})}, \quad (26)$$

where $\sigma_{\min}$ is the smallest singular value. Note also that the eigenvalues of $\tilde{\mathbf{A}}$ are $\lambda_i(\tilde{\mathbf{A}}) = -4+2\cos\left(\frac{i\pi}{N_x+1}\right)$ for $i = 1,..,N_x$ and the eigenvalues of $\hat{\mathbf{A}}$ are $\lambda_i(\hat{\mathbf{A}}) = -3+2\cos\left(\frac{i\pi}{N_x+1}\right)$ for $i = 1,..,N_x$. Furthermore, as $\mathbf{A}$, $\mathbf{B}$ and $\mathbf{I}$ are Hermitian matrices, the following inequalities hold [15],

$$\sigma_{\min}(\mathbf{I}+\mathbf{A}) \geq \sigma_{\min}(\mathbf{I}) + \sigma_{\min}(\mathbf{A}), \quad \sigma_{\min}(\mathbf{I}+\mathbf{B}) \geq \sigma_{\min}(\mathbf{I}) + \sigma_{\min}(\mathbf{B}). \quad (27)$$

Now we can compute the product of the four matrices that conform the matrix iteration $\mathbf{M}$ using the approximations (24) and (25) for the matrices $\mathbf{I} + \Delta t\mathbf{A}_1$ and $\mathbf{I} + \Delta t\mathbf{A}_2$ respectively. Thus,

$$\mathbf{M} \approx \Delta t^2 \begin{pmatrix} \mathbf{B} & & \mathbf{0} \\ & \mathbf{A} & \\ & & \ddots \\ \mathbf{0} & & \mathbf{A} \end{pmatrix}^{-1} \mathbf{D} \begin{pmatrix} \mathbf{A} & & \mathbf{0} \\ & \ddots & \\ \mathbf{0} & & \mathbf{A} \end{pmatrix}^{-1} \mathbf{P}$$

$$= \frac{D_1 D_2 K_1 \Delta t^2}{K_2 \Delta x^4} \begin{pmatrix} \mathbf{B}^{-1} & & \mathbf{0} \\ & \mathbf{A}^{-1} & \\ & & \ddots \\ \mathbf{0} & & \mathbf{A}^{-1} \end{pmatrix} \begin{pmatrix} \mathbf{0} & \mathbf{I} & -\mathbf{I} \\ \mathbf{0} & \mathbf{0} & \mathbf{0} \end{pmatrix} \begin{pmatrix} \mathbf{A}^{-1} & & \mathbf{0} \\ & \ddots & \\ \mathbf{0} & & \mathbf{A}^{-1} \end{pmatrix} \begin{pmatrix} \mathbf{0} & \mathbf{0} \\ \mathbf{I} & \mathbf{0} \end{pmatrix}$$

$$= \frac{D_1 D_2 K_1 \Delta t^2}{K_2 \Delta x^4} \begin{pmatrix} \mathbf{0} & \mathbf{B}^{-1} & -\mathbf{B}^{-1} \\ \mathbf{0} & \mathbf{0} & \mathbf{0} \end{pmatrix} \begin{pmatrix} \mathbf{0} & \mathbf{0} \\ \mathbf{A}^{-1} & \mathbf{0} \end{pmatrix}$$

$$= \frac{D_1 D_2 K_1 \Delta t^2}{K_2 \Delta x^4} \begin{pmatrix} -\mathbf{B}^{-1}\mathbf{A}^{-1} & \mathbf{0} \\ \mathbf{0} & \mathbf{0} \end{pmatrix}.$$

So, we have that

$$\|\mathbf{M}\|_2 \approx \left\| \frac{D_1 D_2 K_1 \Delta t^2}{K_2 \Delta x^4} \begin{pmatrix} -\mathbf{B}^{-1}\mathbf{A}^{-1} & \mathbf{0} \\ \mathbf{0} & \mathbf{0} \end{pmatrix} \right\|_2 = \frac{D_1 D_2 K_1 \Delta t^2}{K_2 \Delta x^4} \|\mathbf{B}^{-1}\mathbf{A}^{-1}\|_2$$

$$\leq \frac{D_1 D_2 K_1 \Delta t^2}{K_2 \Delta x^4} \|\mathbf{B}^{-1}\|_2 \|\mathbf{A}^{-1}\|_2 = \frac{D_1 D_2 K_1 \Delta t^2}{K_2 \Delta x^4} \frac{1}{\sigma_{\min}(\mathbf{A})} \frac{1}{\sigma_{\min}(\mathbf{B})}$$

$$\leq \frac{D_1 D_2 K_1 \Delta t^2}{K_2 \Delta x^4} \frac{1}{1 + \frac{D1\Delta t}{\Delta x^2} |\lambda_i(\tilde{\mathbf{A}})|} \frac{1}{1 + \frac{D2\Delta t}{\Delta x^2} |\lambda_i(\hat{\mathbf{A}})|} \leq \frac{D_1 D_2 K_1 \Delta t^2}{K_2 (\Delta x^2 + D_2 \Delta t)(\Delta x^2 + 2 D_1 \Delta t)},$$

where the last equality holds due to (26) and the previous to last inequality holds by (27).

Therefore,

$$\epsilon := \frac{D_1 D_2 K_1 \Delta t^2}{K_2 (\Delta x^2 + D_2 \Delta t)(\Delta x^2 + 2 D_1 \Delta t)} \longrightarrow \frac{K_1}{2 K_2} \quad \text{when} \quad \Delta x \to 0 \tag{28}$$

is the estimate of $\|\mathbf{M}\|_2$ using the approximations explained above.

5 NUMERICAL RESULTS

First of all we present a numerical solution of the model explained above. Figure 1 shows the initial condition and the discrete solution for $\Delta x = 1/30$, $\Delta t = t_f/10$, $t_f = 0.01$ and $\tau = 1e-4$. One can observe how the absolut maximum of the initial condition decreases with time and the absolut minimum increases. This is due to the heat interaction between both subdomains.

Now we want to compare the estimate ϵ with the convergent rates for different examples varying the thermal diffusivities and conductivities D_1, D_2, K_1 and K_2. Input data for the different cases can be checked in table 1.

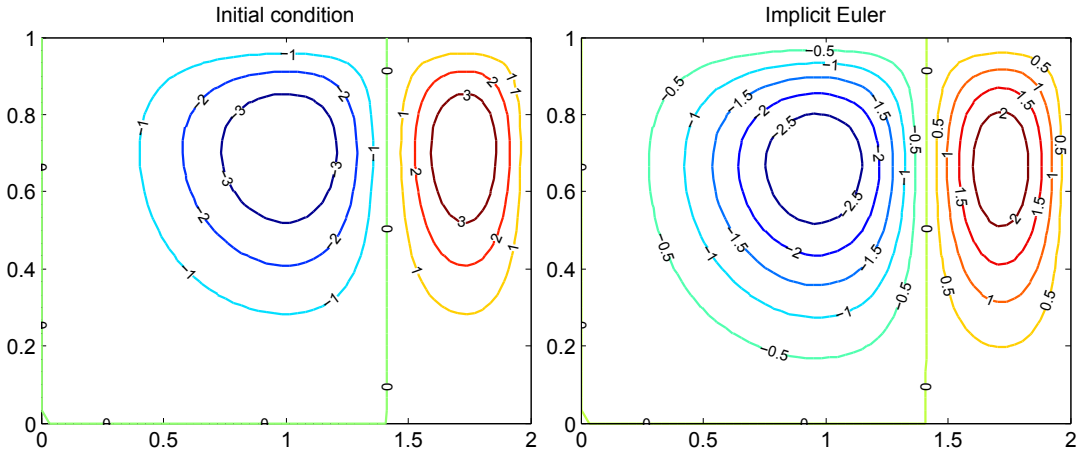

Figure 1: Contour lines of initial condition and discrete solution for $\Delta x = 1/30$, $\Delta t = t_f/10$, $t_f = 0.01$ and $\tau = 1e-4$.

Table 1: Data for different test cases. β is the semi discrete estimate in equation (19), and the last column represents the asymptotics of the discrete estimate ϵ in (28).

Case	D_1	D_2	K_1	K_2	β	$K_1/2K_2$
0	0.1	1	0.1	1	0.32	0.05
1	0.1	0.5	0.2	1	0.45	0.1
2	1	1	1	1	1	0.5
3	0.1	1000	0.1	1	10	0.05
4	1000	0.1	0.1	1	0.001	0.05
5	0.1	1000	1	0.1	1000	5

Figure 2 shows the cases 0, 1 and 2 specified in table 1. We observe that the semidiscrete estimate β is an upper bound and the discrete estimate ϵ intersects at certain point with the convergence rates curve. However, the asymptotic behavior of both estimates is fairly close to the asymptotic behavior of the convergence rates.

Figures 3a and 3b shows the comparison between cases 3 and 4 in table 1. Here, the thermal conductivities K_1 and K_2 are the same in both plots but the thermal diffusivities are switched (meaning that D_1 in case 3 corresponds to D_2 in case 4 and D_2 in case 3 corresponds to D_1 in case 4). We can observe that the asymptotics of the convergence rates do not vary that much in both plots. This pattern is been observed in many numerical experiments when we kept the same values for K_1 and K_2 and we varied D_1 and D_2. This result leads us to the conclusion that the behavior of the convergence rates do not have a strong dependence on the thermal diffusivities D_1 and D_2. This observation matches with the asymptotic behavior of the discrete estimate ϵ (see equation (28)). It is important to notice that the constants D_1 and D_2 have an effect in the convergence rates, but this

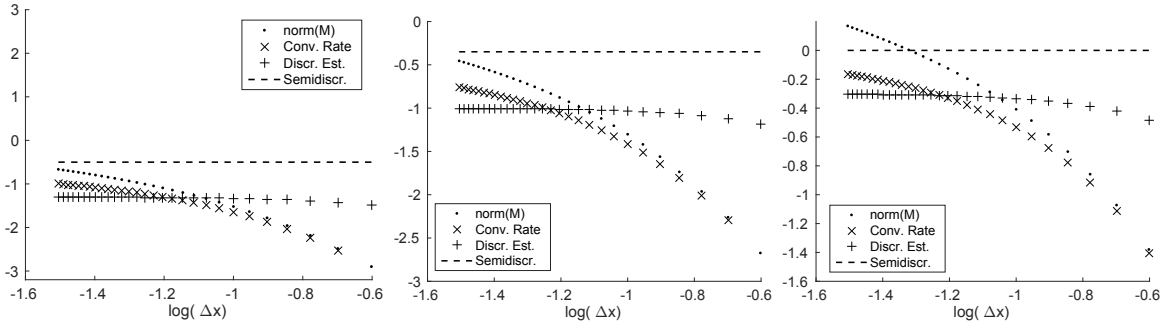

(a) Case 0. (b) Case 1. (c) Case 2.

Figure 2: Cases 0, 1 and 2 from table 1. The dotted line corresponds to $\|\mathbf{M}\|_2$, the dashed line corresponds to the semidiscrete estimate β, the crosses correspond to the discrete estimate ϵ and the remaining line corresponds to the convergence rates. The curves are restricted to the discrete values $\Delta x = 1/30, 1/29, .., 1/2$ and $\Delta t = 0.2$. All the curves are plotted in logarithm scale.

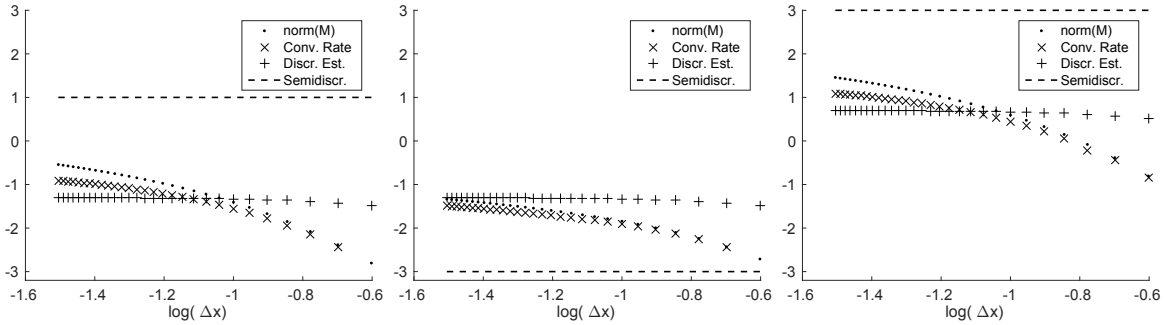

(a) Case 3. (b) Case 4. (c) Case 5.

Figure 3: Cases 3, 4 and 5 from table 1. The dotted line corresponds to $\|\mathbf{M}\|_2$, the dashed line corresponds to the semidiscrete estimate β, the crosses correspond to the discrete estimate ϵ and the remaining line corresponds to the convergence rates. The curves are restricted to the discrete values $\Delta x = 1/30, 1/29, .., 1/2$ and $\Delta t = 0.2$. All the curves are plotted in logarithm scale.

effect vanishes when Δx tends to zero.

The comparison between figures 3a and 3b is also interesting because we can observe a clear difference between the semidiscrete and the discrete cases. In particular, in figure 3a the semidiscrete estimate predicts divergence, but we obtain convergence in the discrete case for all Δx.

Now we see when one keeps the same values for D_1 and D_2 and varies K_1 and K_2. We can see an example of this in figures 3a and 3c where a comparison between cases 3 and 5 is shown. First of all, notice that the plot 3c does not converge, and therefore, the curve named "Conv. Rates" indicates the speed of the iteration in this case. However, although the method does not converge in plot 3c we can observe that ϵ predicts the speed of the iteration well.

Finally, we want to highlight that the experimental convergence rates and $\|\mathbf{M}\|_2$ have

a similiar behavior in figures 2 and 3. However, when Δx tends to zero, $\|\mathbf{M}\|_2$ separates from the convergence rates. This shows that due to the unsymmetry the 2-norm is not a good estimate of the spectral radius when Δx tends to zero.

In conclusion, the main difference observed between the discrete and the semidiscrete cases is that the estimated convergence condition does not depend on the thermal diffusivities D_1 and D_2 for the discrete case.

6 CONCLUSIONS

We have described an approach for solving the coupling of two heat equations on two identical squared domains. In particular, the coupled PDEs were discretized into a system of algebraic equations. Afterwards, a fixed point iteration was performed and the exact iteration matrix was found. And finally, due to the complexity of computing the spectral radius of the iteration matrix, it was approximated by its block diagonal. Numerical results show the accuracy of this approach as well as a comparison between the semi discrete and the fully discrete cases.

The main difference observed between the discrete and the semidiscrete cases is that the estimated convergence condition does not depend on the thermal diffusivities D_1 and D_2 for the discrete case. Moreover, the estimated norm of the iteration matrix is observed to be below the semi discrete estimate β. This proves a faster convergence speed for the fully discrete case than for the semi discrete.

There are a variety of future directions for this work. More complicated domains can be taken into consideration. One can also couple a fluid together with a solid, the so-called fluid structure interaction. Another future direction will be to study the convergence speed of an actual non-linear application.

REFERENCES

[1] Birken, P. Termination criteria for inexact fixed point methods. *Numer. Linear Algebra Appl.*, accepted.

[2] Birken, P., Gleim, T., Meister, A. and Kuhl, D. Fast Solvers for Unsteady Thermal Fluid Structure Interaction. *Int. J. Numer. Meth. Fluids*, submitted.

[3] Buchlin, J.M. Convective Heat Transfer and Infrared Thermography. *J. Appl. Fluid Mech.* (2010) **3(1)**:55–62.

[4] Farhat, C. CFD-based Nonlinear Computational Aeroelasticity. In Stein, E., de Borst, R. and Hughes, T.J.R., editors, *Encyclopedia of Computational Mechanics*, volume 3: Fluids, chapter 13, pages 459-480. John Wiley & Sons, (2004).

[5] Fonseca, C.M. and Petronilho, J. Explicit inverses of some tridiagonal matrices. *Linear Algebra and its Applications.* (2001) **325**:7–21.

[6] Heck, U., Fritsching, U. and Bauckhage, K. Fluid flow and heat transfer in gas jet quenching of a cylinder. *International Journal of Numerical Methods for Heat & Fluid Flow* (2011) **11**:36–49.

[7] Henshaw, W.D. and Chand, K.K. A composite grid solver for conjugate heat transfer in fluid–structure systems. *Journal for Computational Physics.* (2009) **228**:2708–3741.

[8] Hinderks, M. and Radespiel, R. Investigation of Hypersonic Gap Flow of a Reentry Nosecap with Consideration of Fluid Structure Interaction. *AIAA Paper* (2006) **6**.

[9] Kowollik, D.S.C., Horst, P. and Haupt, M.C. Fluid-structure interaction analysis applied to thermal barrier coated cooled rocket thrust chambers with subsequent local investigation of delamination phenomena. *Progress in Propulsion Physics* (2013) **4**:617-636.

[10] Mehta, R.C. Numerical Computation of Heat Transfer on Reentry Capsules at Mach 5. *AIAA-Paper* (2005) **178**.

[11] Meyer, C.D. *Matrix analysis and applied linear algebra*. Siam, (2000).

[12] Quarteroni, A. and Valli, A. *Domain decomposition methods for partial differential equations*. Oxford Science Publications, (1999).

[13] Reuter, M.G. and Hill, J.C. An efficient, block-by-block algorithm for inverting a block tridiagonal, nearly block Toeplitz matrix. *Computational Science and Discovery.* (2012) **5**.

[14] Stratton, P., Shedletsky, I. and Lee, M. Gas Quenching with Helium. *Solid State Phenomena* (2006) **118**:221-226.

[15] Zhang, F. *The Schur complement and its applications*. Springer, (2005).